JOINT EUROPEAN TORUS JET

JET–P(93)58

S.V. Neudatchin, J.G. Cordey, D.G. Muir

The Time Behaviour of the Electron Conductivity during L-H and H-L transitions in JET

The Time Behaviour of the Electron Conductivity during L-H and H-L transitions in JET

S.V. Neudatchin[1], J.G. Cordey, D.G. Muir

JET-Joint Undertaking, Culham Science Centre, OX14 3DB, Abingdon, UK

[1]*Permanent address, IV Kurchatov Institute of Atomic Energy, Moscow, Russia.*

Preprint of a paper to be submitted for publication in
Nuclear Fusion (letters)
July 1993

ABSTRACT

It is shown that during L-H and H-L transitions, soft terminations and strong ELM induced cooling, χ_e changes across most of the JET plasma column on a millisecond time scale (more than a hundred times faster than the energy confinement time τ_E) and usually simultaneously with the evolution of H_α radiation. The speed of response to these transitions is very much faster than previously observed. The jump in the electron conductivity can be easily obtained from experimental data. No scaling $\chi_e(T_e, \nabla T_e)$ can describe the observed electron temperature evolution during the transition. Possible explanations for the jump in χ_e are advanced.

1. INTRODUCTION

Knowledge of the time evolution of local transport coefficients during transitions between various confinement regimes is important in understanding the physical mechanisms responsible for the local transport observed in Tokamak plasmas. This letter reports new observations on the time behaviour of the electron heat diffusivity during some L-H and H-L transitions in JET. Soft terminations and ELMs are also discussed.

An analysis of the time evolution of electron and ion heat diffusivities, χ_e and χ_i respectively, during the L-H transition in JET has been reported previously in [1]. The nature of the transition was clearly seen in the time behaviour of the observed H_α radiation as a slow decay over a ~100 ms period. The transition generally also resulted in a decrease in χ_e and χ_i at inner parts of the plasma column over a longer period of 100 - 300 ms. The time behaviour of the L-H transition varies. Sometimes the decay in the H_α radiation occurs over a few milliseconds. Sub-millisecond decays have also been observed. These observations are consistent with an emerging view that the L-H transition occurs near the plasma edge in a narrow region of width ~ 1 cm on a sub-millisecond time scale. The plasma interior then evolves on a time scale of the order of a confinement time (> 100 ms), much slower than the speed of the transition itself [2]. However, new observations made on JET and reported in this letter show that while there is agreement that the L-H transition occurs very rapidly near the plasma edge, the interior of the plasma responds to the transition on a time scale much faster than a confinement time. Time scales < 5 ms have been observed.

This speed of response has also been seen following the H-L transition, ELMs and soft terminations.

2. THE L-H TRANSITION

As an example of a plasma exhibiting a rapid transition, from L to H, we will examine the JET pulse 26021. Data on the H_α and the local electron temperature behaviour for this hot ion mode 3 MA, 2.8 Tesla discharge with 13 MW of NBI heating and with ∇B drift away from the X-point are shown in Figure 1. The electron temperature, T_e (r,t), was observed with the JET KK2 multi-channel ECE grating polychromator [3]. Temperature data from the spatial region $0.3 \leq r \leq 0.6$ are shown, where r is the normalised minor radius. The L-H transition occurred at time t = 12.39s. The electron temperature profile in the region $r \geq 0.5$ responds immediately to the transition and in the region $r \sim 0.4$, the temperature changes after a delay of a few milliseconds. ($\lesssim$ 5 ms). The rate of change of T_e is typically $\sim 10\ \mathrm{keVs^{-1}}$ following the transition.

The time evolution of the temperature profile is determined by the local electron heat transport and by the local heat sources and sinks. Starting with the equation for conservation of energy,

$$\frac{3}{2}\frac{\partial n_e T_e}{\partial t} = \nabla.\ (Q_e) + P_e \qquad (1)$$

we can examine the possible reasons for the observed rapid response in the electron temperature profile. In equation (1), Q_e is the local electron heat flux ($Q_e = -\chi_e n_e \nabla T_e + \frac{5}{2}\ \Gamma_n T_e$), n_e is the electron density, P_e is the sum of local heat sources and sinks, i.e. $P_e = \Sigma\text{sources} - \Sigma\text{sinks}$, and Γ_n is the electron density flux. Let us write all terms as the sum of a steady value and a perturbed value i.e. $T_e = T_{e_o} + \delta T_e$, $n_e = n_{e_o} + \delta n_e$, $\chi_e = \chi_{e_o} + \delta\chi_e$, etc., and ignoring for now the role of the density flux perturbation, equation (1) becomes

$$\frac{3}{2} n_e \frac{\partial \delta T_e}{\partial t} = \nabla.\ (\delta Q_e) + \delta P_e = -\nabla.\ \left(n_e\left((\chi_{eo} + \delta\chi_e)\nabla\delta T_e + \delta\chi_e \nabla T_{eo}\right)\right) + \delta P_e \quad . \qquad (2)$$

where δQ_e is the electron thermal flux perturbation and δP_e is the perturbation of the electron heat sources and sinks. The relationship $\delta Q_e = -\chi_e^{HP} n_e \nabla \delta T_e$ can be used when $\chi_e \propto \nabla T_e$, because $\chi_e^{HP} = \chi_{eo} + (\partial\chi_e/\partial\nabla T_e)\ \nabla T_e$, where χ_e^{HP} is the

so-called dynamic electron heat diffusivity. The role of the perturbation of density flux $\delta\Gamma_n$ is not obvious, and will be discussed later. It has been assumed that $|\delta n_e/n_e| << |\delta T_e/T_e|$.

We can explain the observed electron temperature behaviour, i.e. the sudden increase in $\partial\delta T_e/\partial t$, as either a decrease of conductive losses or an increase in δP_e or a combination of the two terms. The perturbed heating term δP_e could itself increase either by an increase in the sum of source terms or by a decrease in the sum of sink terms or again by a combination of the two.

For JET pulse #26021, the NBI power was increased about 400 ms before the L-H transition. The injected fast ions would therefore have formed a quasi steady state population by the time the L-H transition occurred and so NBI heating could not directly account for the observed sudden and sustained change in T_e. Similarly, we also believe that impurity radiation inside the flux surface $r \leq 0.6$ also could not be responsible for the observed jump in T_e especially since $T_e \geq 2$ keV. Neither could it have been due to a shifting of the plasma column because soft x-ray data, which independently confirms the ECE data, shows similar behaviour at both inner and outer locations along the plasma mid-plane. While the ion temperature and the axial electron temperature are 11.5 keV and 6.5 keV respectively, and heat flows to the electrons by equilibration, the amount of heating available is insufficient to explain the L-H data. We conclude therefore that the perturbed flux term δQ_e is solely responsible.

Examination of Figure 1 will show that the electron temperature curves, at various positions, increase with similar values of $\partial T_e/\partial t$ and therefore that $\nabla\delta T_e \simeq 0$. This is significant because this means that heat pulse propagation does not occur. This is remarkable given the rapid occurrence of the transition. The perturbed electron heat flux can now be written as $\delta Q_e \simeq -n_e\,\delta\chi_e\,\nabla T_{eo}$, and the term $(\chi_{e_o} + \delta\chi_e)\nabla\delta T_e$ can be ignored, at least in the limited space-time region studied. We conclude that the observed behaviour of T_e is governed by a rapid drop in χ_e, i.e $\delta\chi_e < 0$, and can be described by the equation

$$\frac{3}{2} n_e \frac{\partial \delta T_e}{\partial t} = -\nabla.\ (n_e \delta\chi_e \nabla T_{eo}) \quad . \tag{3}$$

As the temperature profile $T_e(r,t)$ is known, equation 3 can be solved for $\delta\chi_e$. The simplest estimation of $\delta\chi_e$ was obtained by assuming quasi-cylindrical flux surfaces and, by integration, one obtains

$$\delta\chi_e(r_o) = \frac{3}{2}\left(\nabla T_e(r_o) r_o n_e(r_o)\right)^{-1} \int_o^{r_o} n_e \frac{\partial \delta T_e(r)}{\partial t} r dr \qquad (4)$$

For pulse 26021 at $r_o \approx 0.5$ equation 4 gives $\delta\chi_e \approx -0.6\ m^2 s^{-1}$ during the L-H transition. $\delta\chi_e$ generally increase in magnitude with radius.

Another example of the $T_e(r,t)$ evolution after a L-H transition is shown in Fig. 2. This transition occurred in the hot ion mode JET pulse 26064. The plasma parameters before the transition were very close in value to those of pulse 26021 before the transition shown in Fig. 1. However, now the L-H transition was accompanied by a sawtooth crash. We can analyse the decay of the electron temperature perturbation after this crash with the heat pulse propagation method (HPP) described in [4, 5] by assuming that $\partial T_e/\partial t$ changes immediately after the crash to obtain an upper limit to χ_e^{HP}. The value $\chi_e^{HP} \approx 2\ m^2\ s^{-1}$ was obtained.

Let us now examine the possible point of view that the $T_e(r,t)$ variation after the L-H transition in pulse 26021 was caused by a χ_e response to changes in T_e, ∇T_e, i.e. by propagation of a heat wave created by changes at the plasma edge. Assume that the observed electron heating at $r \geq 0.6$ was caused by an unknown mechanism, e.g. a decrease in χ_e and a decrease in plasma radiation. Analysing the "heating" wave propagation with the value of χ_e^{HP} observed, as an upper limit, for the sawtooth crash in pulse 26064, we achieved a fit which is shown by the set of curves 1 in Figure 1. Equation (1) was solved numerically, as in [6] and developed in [7] for pellet induced cooling heat wave studies, with boundary conditions taken from experimental data at $r \approx 0.6$. The calculations show that even with an enhanced value of χ_e the plasma cannot respond very quickly to the L-H transition at the plasma edge.

Of course, calculations made with χ_e^{HP} constant in time are somewhat simplified. One can suggest that calculations made with conductivity varying with gradient and therefore time, i.e. with $\chi_e^{HP} = \chi_{eo} + \alpha\,(\nabla T_{eo} + \nabla\delta T_e)$ can improve the situation. Calculations made with a $\chi_e \propto \nabla T_e$ dependence determined from sawteeth HPP results, do not give a better fit because the value

of ∇T_e decreases in time. The results of these calculations are shown as the set of curves 2 in Figure 1. Again a poor fit was obtained. In conclusion, the observed evolution of T_e during the L-H transition cannot be modelled using heat wave propagation.

Later in pulse 26021 at time $t \approx 12.79$ during a hot ion H-mode ($T_i(0) \approx 15$ keV) and while T_e was increasing, a sawtooth crash occurred. The resulting behaviour of T_e and H_α radiation are shown in Fig. 3. The value of the dynamic electron diffusivity $\chi_e^{HP} \approx 0.6\ m^2\ s^{-1}$ was obtained by the analysis of the decay rate of this perturbation with the method [4]. The low value of χ_e^{HP} represents very good electron confinement (VH mode confinement probably).

Similar low values of χ_e^{HP} were obtained in other very good confinement hot ion H-modes [4, 5]. This observation means that χ_e had decreased below its value immediately after the L-H transition, when χ_e^{HP} was about $2\ m^2\ s^{-1}$, while T_e and ∇T_e increased. Let us suggest the following scenario for χ_e behaviour in this pulse. Initially, in L-mode, χ_e rises quickly with T_e, ∇T_e (χ_e^{HP} increases when ∇T_e, T_e rise in L-mode [4, 5]). Later it drops on a millisecond time scale after the L-H transition. A further gradual decrease in χ_e occurs over a hundred millisecond time scale, similar to the gradual increase in τ_E observed in some other VH discharges on JET [8] and D-III [9].

3. SMALL ELMS AND SOFT TERMINATIONS

It is seen from figure 3 that the slow evolution of T_e after the sawtooth crash in pulse 26021 was interrupted by an ELM. The behaviour of T_e following the ELM could be examined in a similar manner to the L-H transition. By applying equation 4 we concluded that χ_e was increased by $\sim 1\ m^2\ s^{-1}$. Later, both χ_e and the H_α radiation relaxed back to their original H-mode levels.

The evolution of plasma parameters in the JET pulse 26780 (3 MA, 3T, Hot Ion Mode) are shown in Fig. 4. Small ELMs were clearly seen during the stored energy rise phase on both H_α and ECE signals. The values of χ_e^{HP} obtained with the method [4, 5] for two sawtooth crashes during this period were about $0.8\ m^2\ s^{-1}$ and $1.1\ m^2\ s^{-1}$. Variations in H_α were not always correlated with the observable evolution of T_e at inner parts of the plasma. During small ELMs, enhanced levels of H_α exists for about 1-3 ms and the possible χ_e jumps would create small amplitude temperature perturbations only. The effect was smaller

at inner parts of the plasma. Therefore, even small ELMS can influence confinement in the outer region of the plasma column.

A similar picture was seen during the so called "soft-termination" in pulse 26021 which occurred at time t ~ 13.75 (see Figure 5). The NBI power was constant and the sudden jump in Hα radiation was well correlated with the decrease in T_e. We applied equation 4 to give $\delta\chi_e \simeq 1.7\ m^2\ s^{-1}$ at $r \simeq 0.5$ during a period of 10 ms approximately. The corresponding electron power losses were about 8 MW inside $r \leq 0.6$. Later, both χ_e and the H_α radiation relax together.

Assuming the observed cooling at $r > 0.6$ was caused by some unknown effect and analysing the "cooling wave" propagation from $r = 0.6$ with $\chi_e^{HP} = 1\ m^2\ s^{-1}$ (this is an overestimated value of χ_e^{HP} and was determined from sawtooth crashes from pulses with similar very good confinement hot ion H-modes [4, 5]) we achieved the results shown by the set of curves 1 in Figure 5. Curves 2 represent calculations made with $\chi_e = \nabla T_e / \nabla T_{eo}(r)\ m^2\ s^{-1}$, i.e. with χ_e more than double that of the sawteeth induced HPP results. χ_e does not vary gradually in time, but jumps instead during "soft-terminations". This picture is typical and was seen in many similar VH mode pulses.

4. THE H-L TRANSITION

As an example of an H-L transition which was as equally rapid as the L-H transition, electron temperature data for the pulse 26780 is shown in Figure 6. At the time of the transition, $t \approx 14.258$ secs, the NBI power was 6 MW. Using equation 4, the value $\delta\chi_e \approx 0.8\ m^2\ s^{-1}$ at $r \approx 0.5$ was determined. A sawtooth crash occurred later during the L mode at t ~ 14.299 secs. The value $\chi_e^{HP} \approx 3.6\ m^2\ s^{-1}$ was obtained from the analysis of the decay rate of the sawtooth perturbed T_e profile with the method [4, 5].

Modelling of the decay of T_e with $\chi_e(\nabla T_e)$ after the sawtooth crash is shown as the set of curves 1 in Figure 6. A good fit to the data was achieved. Assuming that, for the H-L transition, the observed electron cooling at $r \geq 0.6$ is caused by an unknown mechanism, e.g. an increase in χ_e or an increase in plasma radiation, and analysing the "cooling" wave propagation with the same linear $\chi_e \propto \nabla T_e$ dependence observed for the subsequent sawtooth crash, we achieved a fit to the temperature after the H-L transition which is shown by the earlier set of curves 1

in Figure. 6. Equation 2 was solved numerically with boundary conditions taken from experimental data at $r \approx 0.57$. Clearly a poor fit results.

We also tested the strongly non-linear model $\chi_e \propto (\nabla T_e)^4$. The results are shown as the set of curves 2 in Figure 6. No overall improvement was achieved. This lack of improvement is easy to understand because during the H-L transition there are no significant initial temperature perturbations - the profile evolves slowly in time, with a relatively small amplitude of perturbation. The non-linear component does not contribute much to χ_e, especially during the first 10 ms after the transition.

We can not see any $\chi_e (\nabla T_e, T_e)$ dependency or "heat pinch model" which could describe the $T_e(r, t)$ evolution both during an H-L transition and after the sawtooth crash. The L-H and H-L transitions cannot be described as heat pulse propagation - the electron temperature profile does not evolve as a heat wave.

5. THE L-H AND H-L TRANSITION IN THE PLASMA CORE

Let us now study the central region of the plasma. The $T_e(r, t)$ evolution in this region during the H-L transition of pulse 26021 is shown in Fig. 7. The time delay between channels and the lower values of $\partial Te/\partial t$ at these inner channel positions are clearly seen.

We can attempt to describe the T_e variation in the central region by analysing the "cooling" wave propagation, from the inversion radius, r_{inv}, to the centre of the plasma with boundary conditions taken from experimental data at r_{inv} and with a linear $\chi_e(\nabla T_e)$ dependence. The results of calculations, with $\chi_e \propto \nabla T_e$ about three times less than was determined for the sawtooth crash, are shown as the set of smooth curves, 1, in Figure 7. A good fit was achieved. Thus, a combination of heat pulse propagation and a gradual increase in χ_e, takes place in the central region following the H-L transition.

A similar picture was also seen for the L-H transition and for ELM and soft-terminations. The most natural explanation for the spatial boundary between the conductivity "jump" at $r \geq r_{inv}$ and the more gradual time variation at $r \leq r_{inv}$ is to connect it with the $q = 1$ surface, especially since this boundary is usually located near r_{inv}. A part of anomalous transport outside the $q = 1$ surface could be driven by physical mechanisms other than those inside.

6. THE DENSITY FLUX PERTURBATION TERM

Let us now briefly discuss the possible role of the density and the density flux perturbation in the events described above. Let us suppose that the jumps in the relative value of the electron diffusion coefficient, δD_e, are similar to the jumps in χ_e , i.e. δD_e is proportional to $\delta\chi_e$. Qualitatively, this is seen from experimental data, at least for L-H and H-L transitions when the same trend occurs for the evolution of n_e and T_e, although we have no evidence at the time of writing to suggest that $\chi_e \approx D_e$ or $\delta\chi_e \approx \delta D_e$ on JET. However, if as we believe $|\delta D_e| << |\delta\chi_e|$ then the existence of such a small δD_e would result in a reinforcement of dTe/dt by an approximate factor $(1 + \delta D_e/\delta\chi_e)$ and the values of χ_e obtained before would need to be multiplied by $(1 + \delta D_e/\delta\chi_e)$, i.e. slightly reduced. These corrections can be ignored to first order accuracy.

7. CONCLUSIONS

During L-H and H-L transitions, χ_e is indirectly observed to change very rapidly close to the plasma edge and within a few milliseconds across most of the plasma. H_α radiation usually changes significantly, rapidly and simultaneously with these transitions. The speed of the plasma response is significantly faster than was previously believed which has important consequences for both L and H mode physics. Similar changes to χ_e occur during ELM's and soft terminations. Collectively, these events represent anomalous L-mode transport switching on or off on a millisecond timescale.

Analysis of heat transport showed that only a change in the heat flux was responsible for the observed changes to the electron temperature. There were no significant changes to either heat sources or sinks.

Interestingly, the gradient of the electron temperature profile was not perturbed by these transitions. This enabled the transport equation to be reduced to a simple formula for the change in χ_e after the transition.

The changes in χ_e outside the inversion radius could not be explained by heat wave propagation. No scaling $\chi_e(T_e, \nabla T_e)$ could be found to model the observed changes in T_e. However, the values of $\delta\chi_e$ obtained were in reasonable agreement with the normal L-mode trend i.e. $\delta\chi_e$ rises when T_e, ∇T_e increase. An increase in $\delta\chi_e$ with radius was also observed.

However, the changes in χ_e inside the inversion radius could be explained by heat wave propagation. Therefore, two distinct confinement regions exist. Their boundary is probably the q = 1 surface.

A possible explanation for the χ_e jumps outside r_{inv} is that a part of the anomalous transport is controlled by "noise pumping" created by strong periphery turbulence [10]. Another possible explanation is that a component of the L-mode transport is due to global modes having a large radial scale length.

Indeed, these results add further confirmation to recent experimental observations [11, 12] that L-mode transport is of the "Bohm type" being caused by plasma turbulence which has a radial correlation length scaling with the plasma dimensions.

ACKNOWLEDGEMENTS

The authors wish to acknowledge V.V. Parail and D.J. Campbell for fruitful discussions, together with the JET experimental team for obtaining the data used in this study.

REFERENCES

[1] Balet, B., Cordey, J.G., Stubberfield, P.M., Plasma Phys. and Contrl. Fus., 33 (1991), 1255.

[2] Groebner, R.J., "An Emerging Understanding of H-Mode Discharges in Tokamaks", General Atomics Report: GA-A21128, (1992).

[3] Costley, A.E., Baker, E.A.M., Bartlett, D.V. et al., in Electron Cyclotron Emission and Electron Cyclotron Resonance Heating (Proc. 5th Int. Workshop San Diego, CA, 1985) GA Technologies Inc., San Diego, CA (1985) 3.

[4] Neudatchin, S.V., Muir, D.G., "The study of electron heat transport in JET by analysing the decay of temperature perturbations induced by sawteeth", submitted to Nuclear Fusion. (Rep. JET-P(93) 27, JET Joint Undertaking, Abingdon, Oxfordshire, UK (1993)).

[5] Neudatchin, S.V., Cordey, J.G., Muir, D.G., "A new analysis of sawteeth induced heat pulse propagation and electron conductivity time behaviour during L-H-L transitions on JET" to be published in Controlled Fusion and Plasma Physics, (Proc. 20th Eur. Conf. Lisbon 1993) European Physical Society (1993).

[6] Neudatchin, S.V., Contr. Fus. and Plasma Heating, (Proc. 15th Eur. Conf. Dubrovnik, 1988), V12B, Part III, European Physical Society (1988), 1147.

[7] Bagdasarov, A.A., Borshegovskii, A.A., Vasin, N.L., Elisavetin, A.A., Neudatchin, S.V., Polevof, A.R., Roy, I.N., Savrukhin, P.V., Controlled Fusion and Plasma Heating, (Proc. 17th Eur. Contr. Amsterdam, 1990), V14B, Part I, European Physical Society (1990) 195.

[8] Balet, B., Stubberfield, P.M., Borba, D., et al., "Particle and energy transport during the first tritium experiments on JET", submitted to Nuclear Fusion.

[9] Greenfield, C.M., Jackson, G.L., Burrell, K.H., et al., in Controlled Fusion and Plasma Physics (Proc. 19th Eur. Conf. Innsbruck 1992), vol 16C, Part I, European Physical Society (1992) 11.

[10] Kadomtsev, B.B., Proceeding 19th European Conference on Controlled Fusion and Plasma Physics, Innsbruck, 1992, Plasma Physics and Controlled Fusion 34 (1992) 1931.

[11] Perkins, F.W., Barnes, C.W., Johnson, D.W., Scott, S.D., et al., Phys Fluids B5 1993 477.

[12] Christiansen, J.P., Stubberfield, P.M., Cordey, J.G., Gormezano, C., et al., to appear in Nucl. Fusion.

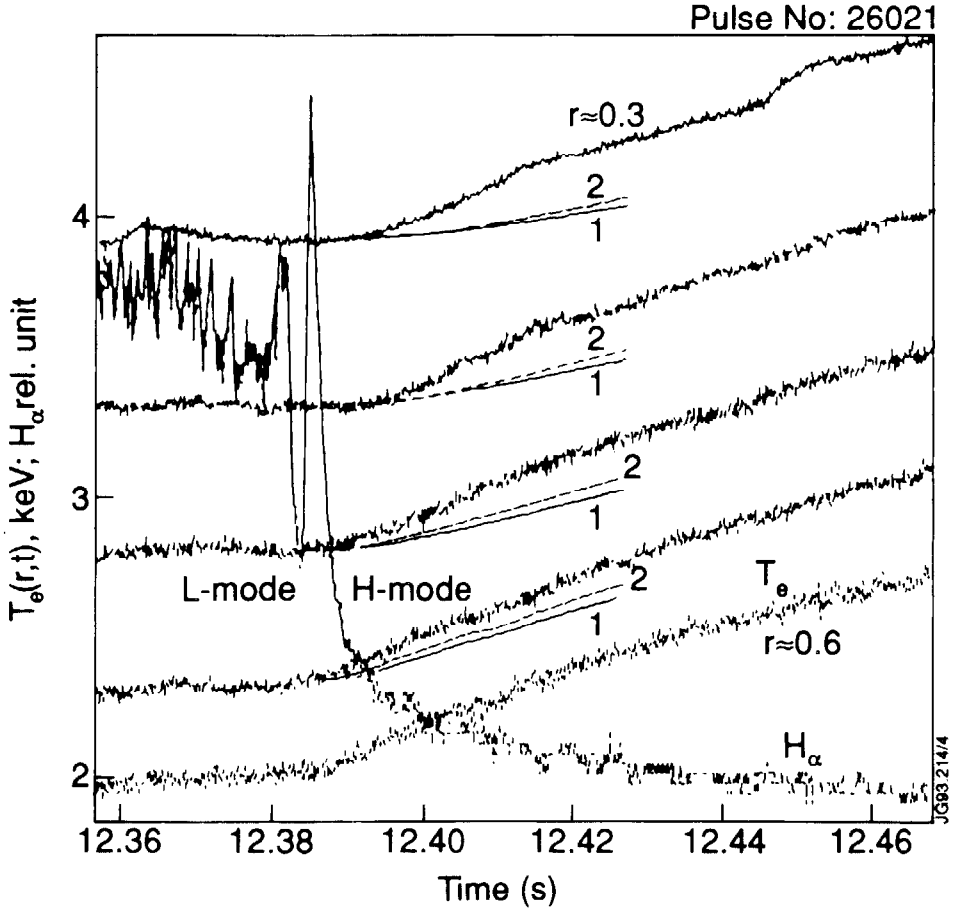

Fig. 1 The evolution of $T_e(r, t)$ and H_α during a L-H transition in pulse 26021 (3.1 MA/2.8T, P_{NBI} = 13 MW). Curves 1 indicate the results from calculations with χ_e^{HP} taken from the analysis of sawteeth induced HPP shown in Fig. 2, and curves 2 are calculations made with χ_e (∇T_e) obtained from the same analysis.

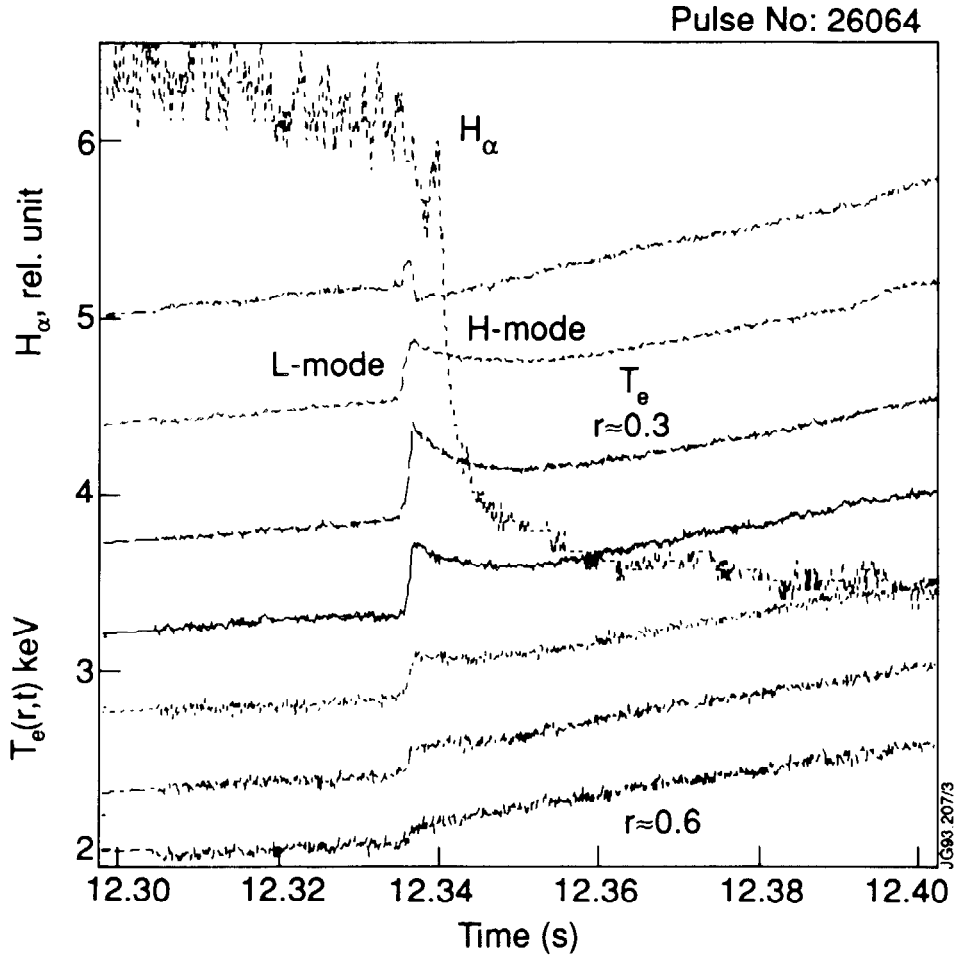

Fig. 2 The evolution of T_e (r,t) and H_α during a L-H transition in pulse 26064. Pulse 26064 is nearly identical to pulse 26021, shown in Fig. 1.

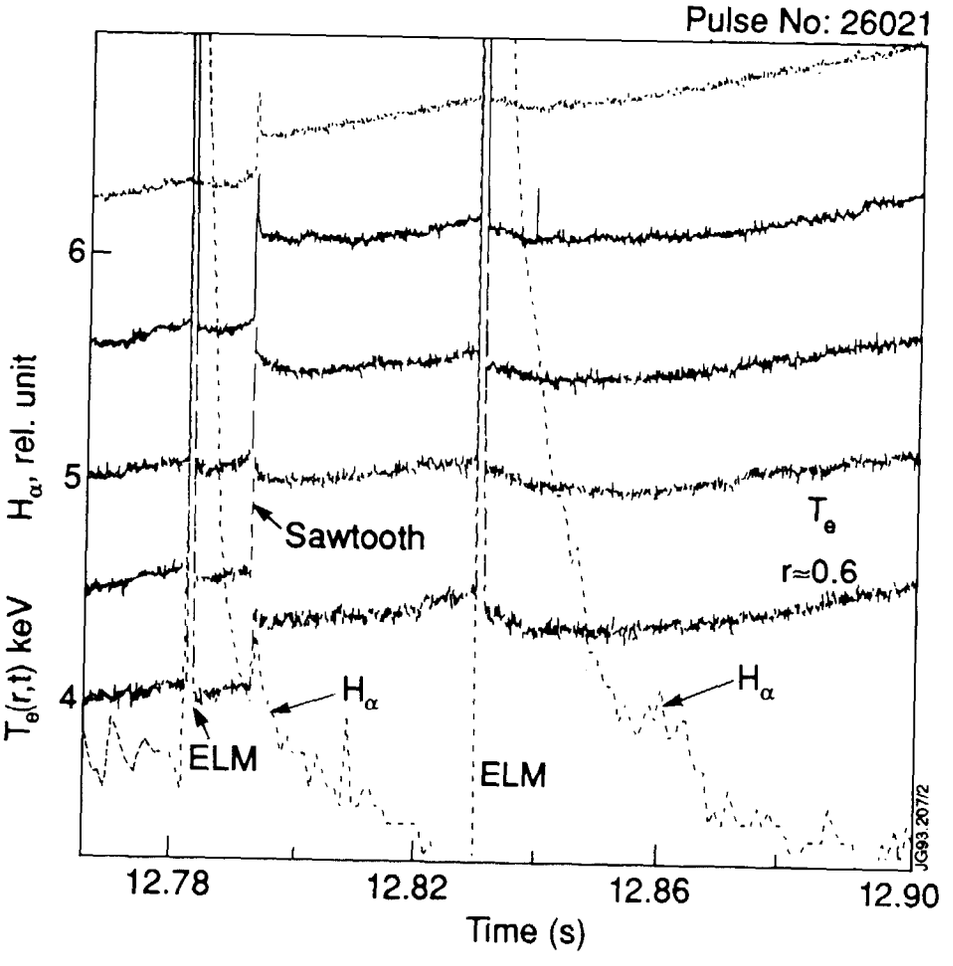

Fig. 3 The evolution of $T_e(r, t)$ and H_α during a sawteeth crash and ELM's in pulse 26021. The temporary destruction of good electron confinement by an ELM is clearly seen.

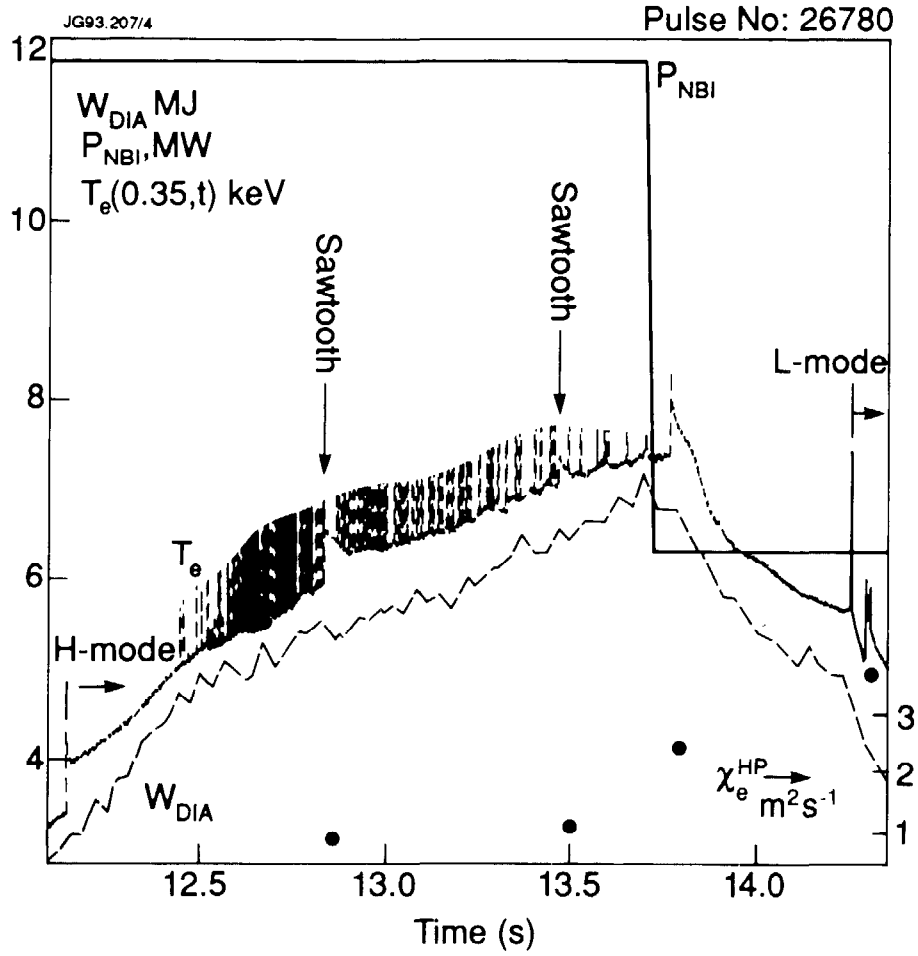

Fig. 4 The evolution of T_e (r,t), P_{NBI} (t), stored energy W(t) and χ_e^{HP} for pulse 26780 (3 MA/3.1T).

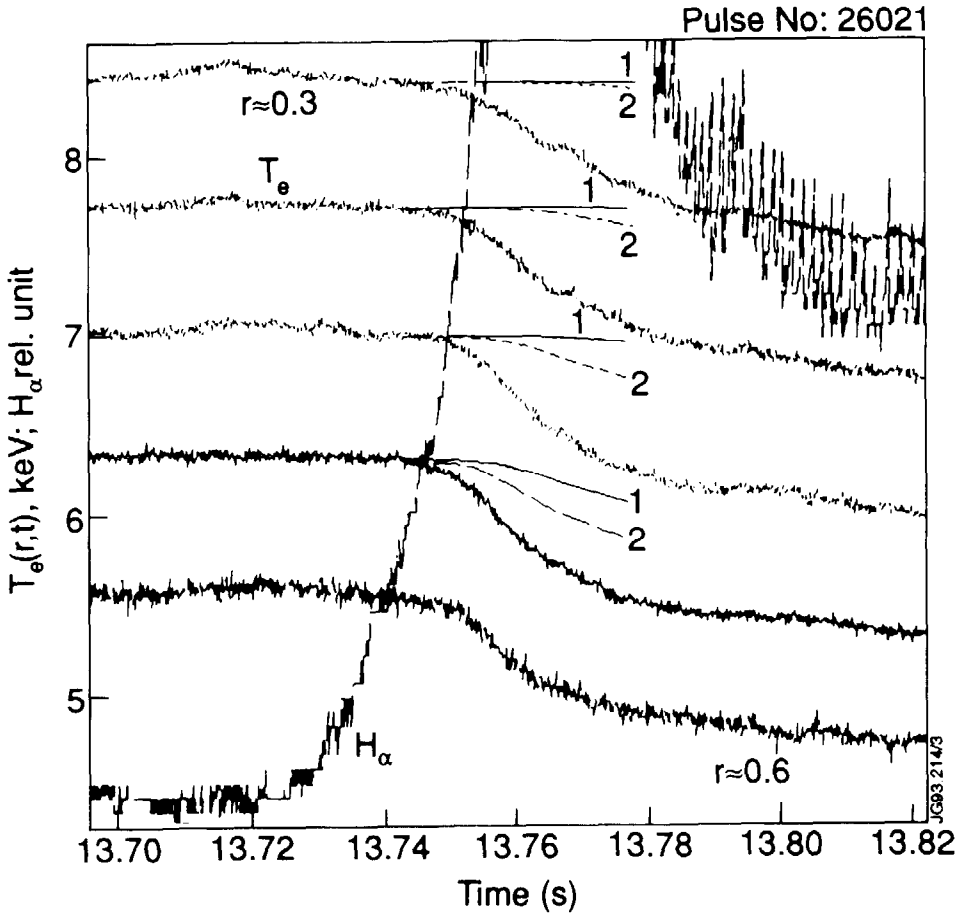

Fig. 5 The evolution of $T_e(r, t)$ and H_α during a Soft Termination in pulse 26021. Curves: 1 indicate the results from calculations with $\chi_e^{HP} = 1\ m^2\ s^{-1}$, typical for sawteeth HPP in VH modes; 2 - calculations with χ_e more than double that of the sawteeth HPP results $\chi_e(\nabla T_e)$ dependence.

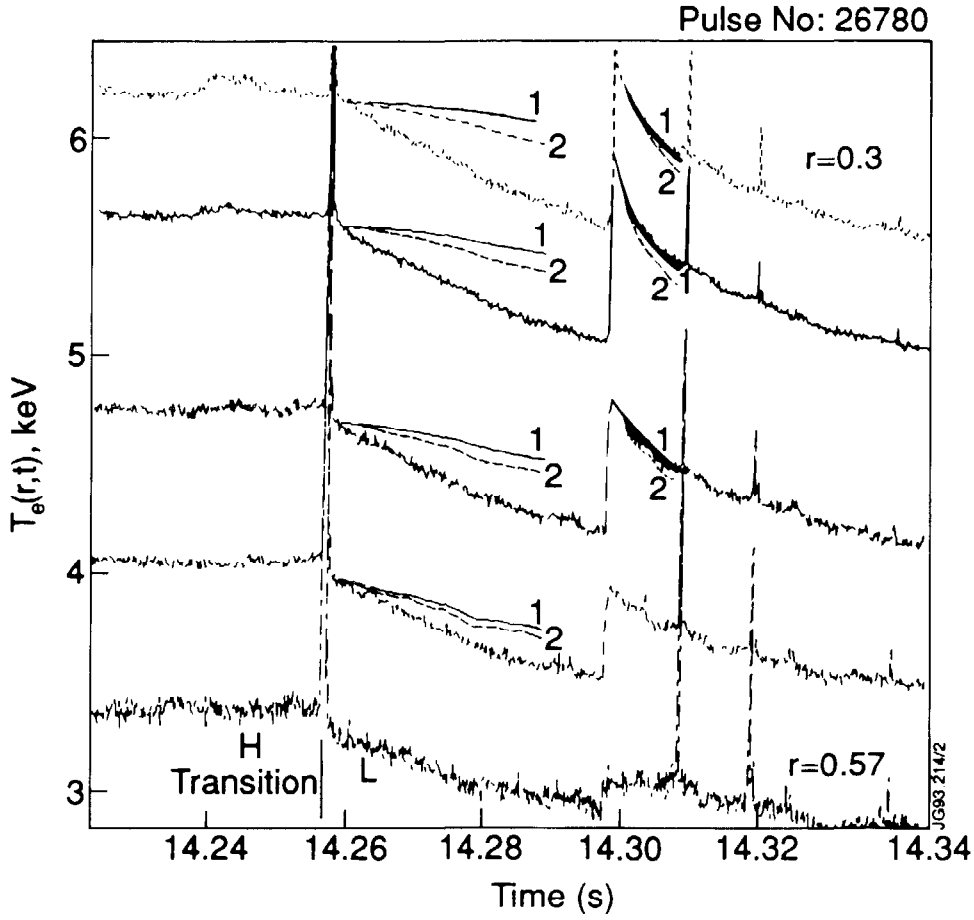

Fig. 6 The evolution of T_e (r, t) during a H-L transition and a sawteeth crash in pulse 26780. Curves 1 and 2 indicate the results from calculations made with a linear χ_e (∇T_e) dependence and a $\chi_e \propto \nabla T_e^4$ dependence respectively.

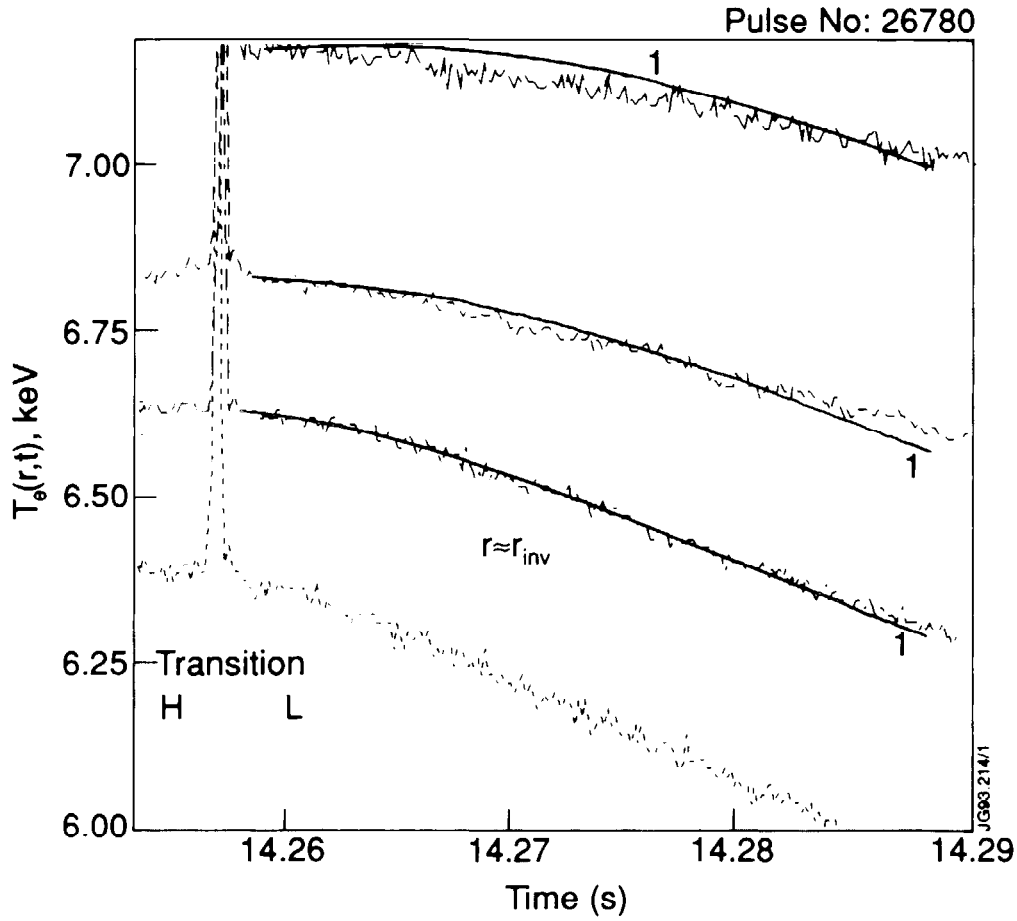

Fig. 7 The evolution of $T_e(r,t)$ during a H-L transition in the central part of plasma column in pulse #26780, curves 1 indicate the results from calculations made with $\chi_e \propto \nabla T_e$ and about 3 times less than was used to calculate the set of curves 1 in Fig. 6.